

Shaping Sparse Rewards in Reinforcement Learning: A Semi-supervised Approach

Wenyun Li¹, Wenjie Huang²

¹Department of Mathematics, The University of Hong Kong, Hong Kong SAR

²Department of Data and Systems Engineering, The University of Hong Kong, Hong Kong SAR

²Musketeers Foundation Institute of Data Science, The University of Hong Kong, Hong Kong SAR
wenyunli@hku.hk

Abstract

In many real-world scenarios, reward signal for agents are exceedingly sparse, making it challenging to learn an effective reward function for reward shaping. To address this issue, the proposed approach in this paper performs reward shaping not only by utilizing non-zero-reward transitions but also by employing the *Semi-Supervised Learning* (SSL) technique combined with a novel data augmentation to learn trajectory space representations from the majority of transitions, i.e., zero-reward transitions, thereby improving the efficacy of reward shaping. Experimental results in Atari and robotic manipulation demonstrate that our method outperforms supervised-based approaches in reward inference, leading to higher agent scores. Notably, in more sparse-reward environments, our method achieves up to twice the peak scores compared to supervised baselines. The proposed double entropy data augmentation enhances performance, showcasing a 15.8% increase in best score over other augmentation methods.

Introduction

The sparse reward problem is a core challenge in Reinforcement Learning (RL) when solving real-world tasks (Kober, Bagnell, and Peters 2013). In supervised learning, supervision signals are provided by the training data. In reinforcement learning, rewards take on the role of supervision signals, guiding the agent to optimize its policy. Many real-world tasks naturally have the feature of delayed or infrequent rewards due to the complexity and nature of the tasks. In tasks like Go (Silver et al. 2016), navigation (Wang et al. 2020), or robotic arm manipulation (Gu et al. 2017; Riedmiller et al. 2018), agents only receive rewards upon successfully achieving the final goal, such as winning a game, reaching a target, or completing a grasp, with no feedback for intermediate steps. Sparse reward provides little immediate feedback to guide the agent’s exploration and high variance in returns, makes it difficult to learn the optimal policy (Plappert et al. 2018).

A potential solution to tackle the sparse reward problem is *reward design and learning* (Ng, Harada, and Russell 1999). Methods in this category often operate on the replay buffer, processing off-policy data to implement their respective reward design (Schaul et al. 2015; Andrychowicz et al. 2017; Peng et al. 2019). Pathak et al. (2017) propose the Intrinsic Curiosity Module (ICM) that formulates curiosity as the

error in an agent’s ability to predict the consequence of its own actions learned by a self-supervised inverse dynamics model. However, curiosity-driven methods face a significant challenge: curiosity, as an intrinsic reward, is inherently decoupled from the actual objectives and tasks. This may cause agents to overly focus on “new” but meaningless states. Kumar, Peng, and Levine (2019) propose Reward Conditioned Policy (RCP) that uses supervised learning as an incentive, thereby eliminating reliance on manually designed novelty as the objective. Building upon this, Self-Supervised Online Reward Shaping (SORS, Memarian et al. (2021)) formalizes a self-supervised learning framework and apply it to sparse-reward environments. In SORS, the original sparse reward provides a self-supervisory signal for reward inference by ranking trajectories that the agent observes, while the policy update is performed with the newly inferred, typically dense reward function. However, methods based on non-expert trajectories under supervised learning suffer from poor sample efficiency (Peng et al. 2019), especially when non-zero-reward transitions are extremely rare in sparse reward cases.

In order to bridge the gap in handling sparse rewards, our approach performs reward shaping not only by utilizing non-zero-reward transitions but also by employing *Semi-Supervised Learning* (SSL) technique to learn trajectory space representations from the majority of transitions, i.e., zero-reward transitions, thereby improving reward shaping. Explicitly, we propose an RL algorithm that applies the idea of SSL, called Semi-Supervised Reward Shaping framework (SSRS), and also propose a new data augmentation technique called double entropy data augmentation applied on non-image transitions as the perturbation method for SSL. By progressively approximating the state-value function and the action-state function in the reward estimator, we shape the reward in sparse-reward trajectories. Consistency regularization to both zero-reward and non-zero-reward transitions is adopted for the optimization of the reward estimator. Additionally, a monotonicity constraint is incorporated over the two components of the reward shaping estimator to further reduce the discrepancy between the shaped reward distribution and the true reward distribution.

We evaluate the performance of SSRS in reward-sparse Atari and robotic manipulation environments, comparing it with SORS (Memarian et al. 2021), RCP (Kumar, Peng, and Levine 2019) methods. Our model demonstrates perfor-

mance superior than other supervised-based approaches and achieves a maximum increase over RCP by a factor of two in reaching higher best scores. We further validate that the proposed double entropy data augmentation enhances performance showcasing a 15.8% increase in best score compared to other augmentation methods.

Related Work

There are different reward shaping methods for different objectives: Count-based methods (Choi et al. 2019; Ostrovski et al. 2017; Bellemare et al. 2016) incentivize agents based on the rarity of states, while curiosity-driven exploration methods reward the agent’s exploratory behavior. ICM Pathak et al. (2017) also pursues rarity, but operationalizes it by defining curiosity as the error in the agent’s ability to predict the consequences of its own actions in a visual feature space. This curiosity signal serves as an intrinsic reward, driving the agent to explore novel states. Andrychowicz et al. (2017) propose Hindsight Experience Replay (HER) that enables learning from failures by treating unachieved goals as alternative goals for experience replay.

Approaches using supervised learning for reward shaping don’t rely on specific objectives. The study (Kumar, Peng, and Levine 2019) employs *supervised learning* techniques, viewing non-expert trajectories collected from sub-optimal policies as optimal supervision to do the reward shaping. Memarian et al. (2021) leverage self-supervised methods to extract signals from trajectories while simultaneously updating the policy.

We extend supervised learning to a semi-supervised paradigm and introduce SSL techniques into the RL framework, specifically employing *consistency regularization* and *pseudo-labeling* (Bachman, Alsharif, and Precup 2014) in the trajectory space. In the realm of SSL, *consistency regularization* leverages unlabeled data by capitalizing on the invariance assumption—that the model should yield consistent predictions when presented with perturbed variants of identical inputs. Berthelot et al. (2019); Sohn et al. (2020) further improve this methodology on image classification tasks. *Pseudo-labeling* (Lee 2013) utilizes the model’s predicted hard labels (obtained via arg max operations) for unlabeled data, retaining only those predictions whose confidence scores \mathbf{q} exceed the threshold τ , and optimizes them via:

$$\mathcal{L}_u = \mathbb{1}(\max(\mathbf{q}) \geq \tau) \cdot \mathcal{H}(\mathbf{q}, \arg \max(\mathbf{q})). \quad (1)$$

Note we directly write \mathbf{q} , omitting the dependence of \mathbf{q} on the parameters and $\mathbb{1}(\cdot)$ is the indicator function.

Another related direction is the application of data augmentation for trajectories (Shorten and Khoshgoftaar 2019) in RL algorithms (Yarats, Kostrikov, and Fergus 2021). Most of them process image data to enhance the agent’s generalization performance. Hansen and Wang (2020) decouple augmentation from policy learning and is found to significantly advance sample efficiency, generalization, and stability in training over vision-based RL methods. Yarats et al. (2022) use data augmentation to learn directly from pixels and is able to solve complex humanoid locomotion tasks directly from pixel observations. Studies like Lin et al. (2019)

generate feasible trajectories based on symmetries observed in the trajectory space for robot control tasks, thereby constructing an Invariant Transform Experience Replay framework to address the issue of high sample requirements.

Methodology

In this section, we introduce the proposed method and its pipeline is graphically illustrated in Figure 1, which consists of two components: a reward estimator optimized through semi-supervised learning, and a reward estimator optimized through semi-supervised learning and the data augmentation technique for zero-reward transitions that serves as the perturbation required for semi-supervised learning. We will elaborate the key parts of the method in the following subsections and the detailed steps are shown in Algorithm 1.

Semi-Supervised Reward Estimator

The reward estimator is the very module that takes (augmented) transitions as input and outputs estimated rewards (see Figure 1). During the training phase, the estimator is optimized via consistency regularization using the cross-entropy. In the prediction phase, the final estimated reward is generated through arg max selection, choosing the z value corresponding to the peak of the confidence score distribution. The SSRS framework proposed in this paper, aims to fit an optimal state-value function $V^*(s)$ and an optimal action-value function $Q^*(s, a)$, which are used to shape the rewards of trajectory. Note we use $Q(s, a)$ and $V(s)$ to denote aforementioned function before parameter optimization. Given an one-step trajectory $\langle s_t, a_t, r_t, s_{t+1} \rangle$, the estimated reward can be calculated from the estimations of the state-value function $V(s)$ and the action-value function $Q(s, a)$ as follows. We first define the confidence score vector of timestep t over a fixed reward set $Z = \{z_i, i = 1, \dots, N_z\}$ in Eq.(2), where N_z is a hyperparameter controlling the number of estimated rewards. The value of fixed reward set is initialized according to the collected true reward value, and is updated throughout the process of agent’s interactions with environment.

By the following Eq.(2), we can get confidence vector $\mathbf{q}_t \in \mathbb{R}^{N_z}$ at timestep t , with each element $q_i \in \mathbf{q}_t$ corresponding to a estimated reward $z_i \in Z$, computed as

$$\mathbf{q}_t = \beta Q(s_t, a_t) + (1 - \beta) V(s_{t+1}). \quad (2)$$

The reward z estimated from the trajectory $\langle s_t, a_t, r_t, s_{t+1} \rangle$ essentially evaluates the quality of the agent’s interaction with the environment at the current step based on the trajectory. We utilize $Q(s_t, a_t)$ to assess the long-term return (*i.e.*, the cumulative future reward) of taking action a_t in state s_t , and combine this with the future cumulative return estimation $V(s_{t+1})$ of transitioning to state s_{t+1} after taking action a_t in state s_t , which gives us the estimated z in the form of linear combination of the two, with $\beta > 0$. The estimate reward value z_t is selected with maximum confidence score above the threshold λ , *i.e.*, $z_t = \alpha(\mathbf{q}_t, \lambda)$, where

$$\alpha(\mathbf{q}_t, \lambda) = \begin{cases} \arg \max_{z_i} \mathbf{q}_t, & \text{for } q_i > \lambda, i = 1, \dots, N_z, \\ 0, & \text{else.} \end{cases}$$

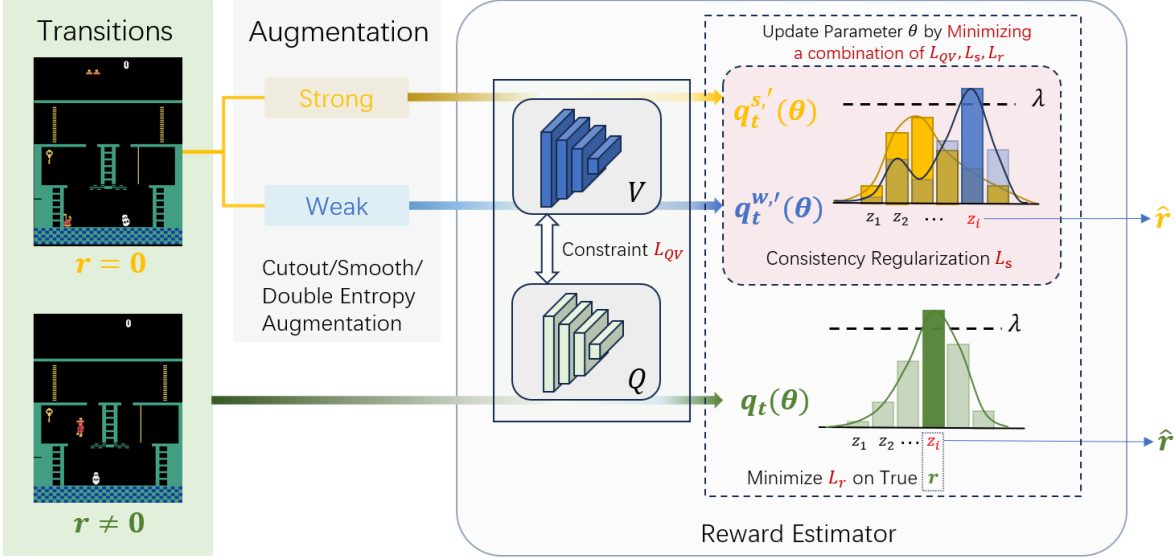


Figure 1: The figure illustrates how the SSRS method leverages both non-zero reward transitions and sparse reward transitions for reward shaping through a semi-supervised learning (SSL) approach incorporating strong-weak data augmentation. The augmentation techniques include Cutout, Smooth, and Double Entropy Augmentation, among others (see Table 2 in the Appendix for details).

Note that we will use $q_t(\theta)$ in subsequent sections to explicitly denote its dependence on θ , which consists of θ_1 (the parameter of the Q function) and θ_2 (the parameter of the V function). During the prediction stage, we apply shaping to a proportion p_u of transitions in the buffer, where p_u dynamically adjusts throughout training. Specifically, p_u is initially set proportional to $\log(\mathcal{N}_r)$, then increased to match \mathcal{N}_r during the mid-training phases, before being reduced again to scale with $\log(\mathcal{N}_r)$. Here, \mathcal{N}_r represents the count of trajectories containing genuine reward signals. This prevents excessive variance in the initial policy gradient updates or Q -network updates, while in later stages, phases out reliance on shaped rewards as the policy converges toward optimal behavior.

In order to obtain the optimal θ value for accurately estimating the reward value of each trajectory $\langle s_t, a_t, r_t, s_{t+1} \rangle$, SSRS framework first optimizes the following loss function using only transitions with non-zero rewards, so as to minimize the discrepancy between the reward estimator's predictions and the ground truth values for these transitions. The handling of zero-reward transitions will be addressed in consistency regularization section.

$$L_r = \frac{1}{\mu B} \sum_{t=1}^{\mu B} \mathbb{1}(\max(q_t(\theta)) \geq \lambda) (r_t - \alpha(q_t(\theta), \lambda))^2. \quad (3)$$

Note that μ represents the proportion of non-zero rewards in the buffer, which quantifies the sparsity level, and B is the batch size of trajectories.

Monotonicity Constraint Since the estimator employs two neural networks, we introduce a constraint to regulate

their outputs and stabilize the training process. The value function $V(s_t)$ provides a global baseline for a state, while advantage function captures the relative advantage or disadvantage of action a with respect to this baseline. This separation makes it easier to assess the relative importance of specific actions, and thus compensates for the insensitivity to actions because the disturbance of data augmentation only takes place on state s . By utilizing the relationship between V and Q , we can introduce the monotonicity constraint in the SSRS framework as follows, which quantifies the mean square positive advantage function values. Define advantage function $\delta_t(\theta) = Q(s_t, a_t, \theta_1) - V(s_t, \theta_2)$ where θ is the combination of θ_1 and θ_2 , we have

$$L_{QV} = \begin{cases} 0, & \delta_t(\theta) < 0, \\ \frac{1}{\mu B} \sum_{t=1}^{\mu B} (\delta_t(\theta))^2, & \text{else.} \end{cases} \quad (4)$$

Minimizing the objective loss L_{QV} over the parameter θ of can achieve a more stable update, which will be validated in experiment section, and is crucial to SSRS framework's success.

Consistency Regularization Consistency regularization is a paradigm in the field of SSL (Sajjadi, Javanmardi, and Tasdizen 2016), and is also the key to optimize the reward estimator with the limited feedback reward signal in the sparse reward trajectories. The reward estimator, as a crucial component in SSRS, needs to capture the invariance of trajectories, which refers to the estimated reward unaffected by minor variations in input transitions, aligning with the characteristics of consistency regularization. Furthermore, in scenarios with sparse rewards, applying weak

strong augmentations to transitions with zero and non-zero reward transitions before conducting consistency regularization further enhances the generalization ability of the reward estimator in sparse reward environments.

The weak and strong augmentations refer to Table 2 in Appendix, where we consider Gaussian noise with smaller parameters as weak augmentation, and other augmentation such as smoothing, translation, and cutout, with larger parameters as strong augmentation. In conventional data augmentation for weak-strong augmentation, standard techniques such as cutout, flipping, and rotation are typically employed. The unitless property of Entropy makes it particularly useful in data augmentation, as it allows for a fair comparison of information content across different features, regardless of their scale or domain. Entropy is essentially a measure of uncertainty or randomness in a probability distribution, and it is calculated in a way that normalizes the result, making it dimensionless. Building on this intuition, we further adapt a novel double entropy data augmentation method to serve in SSRS on non-image tasks. The implementation details are provided in Appendix.

More specifically, for transitions with zero rewards, the reward estimator computes the loss as shown in Eq.(5), which is the loss between the strong augmentation term and weak augmentation term following typical loss design in consistency regularization. Assuming continuity of trajectories in the metric space, it calculates the confidence of reward values after weak and strong augmentations, denoted by \mathbf{q}_t^w and \mathbf{q}_t^s , respectively. The calculation of \mathbf{q}_t^w and \mathbf{q}_t^s follows Eq.(2), simply replacing the input state s with its weakly or strongly augmented version. Here we omit their dependence on θ for simplicity. For confidence values greater than the threshold in weak augmentation, the one-hot operation is performed (Bachman, Alsharif, and Precup 2014), denoted as $\mathbf{q}_t^{w,'}$, and then used to compute the cross-entropy loss with the normalized confidence values greater than the threshold in strong augmentation, denoted as $\mathbf{q}_t^{s,'}$. The loss function is denoted as.

$$L_s = \frac{1}{(1-\mu)B} \sum_{t=1}^{(1-\mu)B} [\mathbb{1}(\max(\mathbf{q}_t^s) \geq \lambda, \max(\mathbf{q}_t^w) \geq \lambda) \cdot \mathcal{H}(\mathbf{q}_t^{w,'}, \mathbf{q}_t^{s,'})], \quad (5)$$

where \mathcal{H} denotes the cross-entropy.

The algorithm for value-based SSRS with synchronous update—*i.e.*, *value function update and reward shaping carry out simultaneously*—is outlined in Algorithm 1. The agent begins by collecting experience transitions. The reward estimation network is then initialized through back-propagation, which can be performed either synchronously or asynchronously using the loss function. The complete SSRS loss function, as specified in Eqs. (3), (4) and (5), combines these components through the weighting parameter α . In Appendix, we provide the derivations of the “approximate” gradients of loss functions L_{QV} , L_r and L_s with respect to θ in Appendix, after approximating the indicator functions by sigmoid function.

Algorithm 1: Value-based SSRS Framework

Parameter Confidence threshold λ , loss weight α , set Z with size N_z , episodes T , update probability p_u ;

```

1: Initialize parameters  $\theta$ ,  $Q$  function, replay buffer  $\mathcal{D}$ ;
2: for  $t = 1$  to  $T$  do
3:   repeat
4:     Take  $a_t$  from  $s_t$  using policy derived from  $Q$  (e.g.,  $\epsilon$ -greedy), observe  $r_t$ ,  $s_{t+1}$ 
5:     if  $r_t \notin \{r_1, \dots, r_{t-1}\}$  then
6:       Obtain  $N_z$  new  $z_i$  by interpolating from all historical observation  $r_1, \dots, r_t$ 
7:     end if
8:     if  $r_t = 0$  then
9:       Calculate confidence  $\mathbf{q}_t(\theta)$ ,  $\mathbf{q}_t^{w,'}(\theta)$  of non-zero and zero reward transitions over set  $Z$  under parameter  $\theta$ .
10:      Perform reward shaping on zero-reward transitions in  $\mathcal{D}$  of the  $p_u$  ratio.
11:    end if
12:    Choose a batch of transitions  $\mathcal{B}$  from  $\mathcal{D}$  and update  $Q$  function with shaped reward  $\hat{r}$ ,
13:    until  $s_{t+1}$  is the terminal state
14:    Update parameter  $\theta$  through minimizing the objective

$$L = L_{QV} + \alpha L_s + (1 - \alpha) L_r$$

15: end for

```

Experiment Results

The experiments aim to validate whether the SSRS using semi-supervised learning is more efficient in reward shaping than the self-supervised method, thereby improving the best score achieved by the agent in both the Atari game environment (Bellemare et al. 2013) and the robotics manipulation environment (Plappert et al. 2018) (see Figure 2). To demonstrate the superiority of double entropy data augmentation over other data augmentation methods in non-visual observation tasks, we use Random Access Memory (RAM) as the observation. Additionally, ablation experiments are conducted to demonstrate the importance of monotonicity constraints in the application of SSL techniques. We will analyze the characteristics of the trajectory space through experiments to provide insights into the underlying reasons of such improvement.

Experimental Setup. RAM observation refers to a representation of the Atari RL environments’ internal state directly from its Random Access Memory, typically 128 bytes of RAM (*i.e.*, a vector of 128 integers, each in the range [0, 255]). The implementation for this experiment is based on the Tianshou RL library (Weng et al. 2022). Across three experimental seeds, a maximum of 2000 transition samples per episode are collected and appended to the buffer \mathcal{D} , a

buffer with a capacity of 30k transitions. The maximum test score achieved from the start of training up to the current epoch, along with its variance across different experimental seeds, is recorded and plotted in the figures throughout this section. Some of the hyperparameter settings are as Table 4 in Appendix, which are determined based on preliminary hyperparameter tuning results, and consistent hyperparameter settings are used in both the Robotics and Atari experiments.

Performance of SSRS

To evaluate the proposed SSRS framework, we compare it with several baseline approaches including supervised-based methods (RCP (Kumar, Peng, and Levine 2019) and SORS (Memarian et al. 2021)) as well as backbone reinforcement learning algorithms in both Atari and robotic environments. Since this paper focuses on reward shaping, the backbone algorithms used are not the main emphasis. The backbone algorithms for Atari and Robotic environments are Soft Actor-Critic (SAC, Haarnoja et al. (2019)) and Deep Deterministic Policy Gradient (DDPG, Lillicrap et al. (2015)), respectively. Several variants of the SSRS framework are employed, including SSRS-S, which uses double entropy augmentation, SSRS-C, which adopts the cutout method for data augmentation, and SSRS-M, which adopts the smooth method for data augmentation.

In Atari environment, the SSRS algorithm and its variants outperform the baseline algorithm and supervised-based RCP across all four games (see Figure 3). This is because When the proportion of transitions with non-zero rewards is low (i.e., when μ is small), the self-supervised method has fewer samples containing "ground truth labels" available for learning. In such cases, the SSRS approach, which leverages semi-supervised learning to infer trajectory decision boundaries, can estimate rewards from transitions more effectively than the self-supervised method. (The concept of trajectory decision boundaries will be discussed in section 'Feasibility of Semi-Supervised Learning'.) Seaquest and Hero games are considered to be moderately reward-sparse, so we add them to the setting to evaluate the general performance of SSRS. In terms of convergence speed, the SSRS-S variants

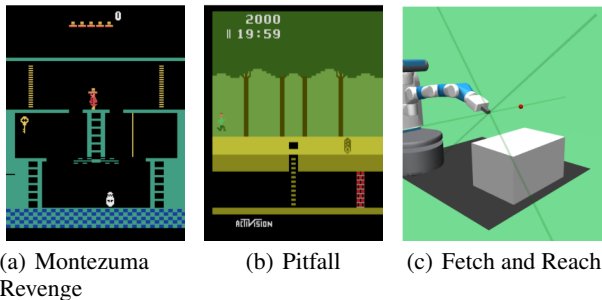


Figure 2: (a) and (b) show the game scenes from Montezuma Revenge and Pitfall as Sparse reward environment of the Arcade Learning Environment (ALE), commonly referred to as Atari. (c) is a snapshot of robotic arm performing Fetch and Reach task in Gymnasium-Robotics environment.

Table 1: Average best score of SSRS framework with monotonicity (SSRS-ST) constraint and without monotonicity constraint (SSRS-NST) in 4 environments (mean \pm std over 3 seeds).

AVG BEST SCORE	SSRS-ST	SSLRL-NST
SEAQUEST	476.6 \pm 85	447.5 \pm 18.9
HERO	8825 \pm 2317	7596.6 \pm 81.4
MONTEZUMA	166.6 \pm 104	100 \pm 70.7
VENTURE	200 \pm 0	262.5 \pm 47.9

outperform RCP in the Venture environment. Moreover, in games with extremely sparse rewards, such as MonteZumaRevenge, SSRS significantly outperforms the RCP algorithm, achieving nearly 2 times the best score in MonteZumaRevenge (see Figure 3(c)). In the FetchReach environment in Robotics, where the reward signal is binary, i.e., the reward is -1 if the end effector hasn't reached its final target position, and 0 if the end effector is in the final target position, the SSRS framework outperforms the self-supervised method SORS (see Figure 4).

We also conduct experiments to evaluate the performance of SSRS when using different data augmentation methods as perturbations for SSL, aiming to investigate whether the proposed double entropy data augmentation provides greater improvement in terms of final best score for SSRS compared to other traditional data augmentation methods (e.g., flip, scale, translate). The detailed results and analysis are provided in Appendix.

Ablation Experiments of Monotonicity Constraint

We conduct a series of experiments on the SSRS framework under conditions with and without monotonicity constraint and study the distribution of reward values at different stages of training in both scenarios.

The average best score obtained is presented in Table 1. In three environments, SSRS with a monotonicity constraint achieves higher best scores compared to SSRS without a monotonicity constraint. We find that adding the monotonicity constraint reduces the variance as well as the final best score in reward-sparse environments with long-term goals (see Figure 3 and 1 in Appendix). One of the reasons of such difference in sparse and less-sparse scenarios is our strategy of configure in update probability p_u . The hyperparameter p_u is set proportional to the number of non-zero-reward transitions, \mathcal{N}_r . However, the variation in the number of non-zero-reward transitions across different environments is not linear. Although we improved the method by setting p_u to the order of $\log(\mathcal{N}_r)$ during the early stages of training, this adjustment does not cover all possible scenarios.

Further investigation of the reward distribution in Hero (see Figure 5) reveals that, according to the reward distribution of the backbone algorithm without reward shaping, most of the reward signals in this environment consist of small reward values, with a lack of medium to long-term reward feedback. SSRS without a monotonicity constraint only provides reward estimates close to the mean. However,

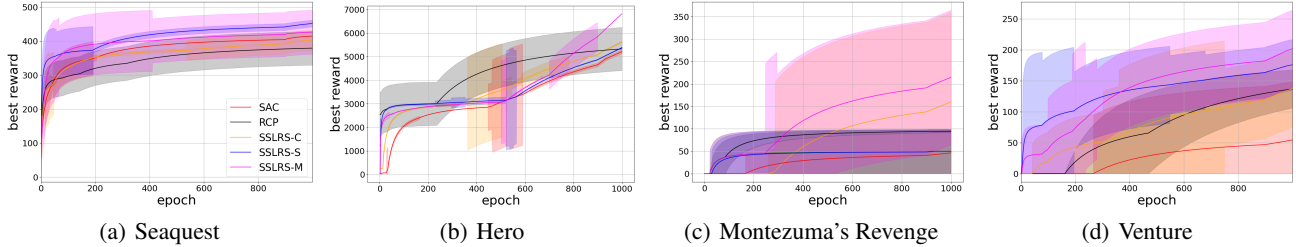


Figure 3: Figures (a-d) demonstrate the best score in 1000 epochs of different algorithms in 4 Atari environments (mean \pm std over 3 seeds). Different curves represent the SSRLS framework and its variants, as well as RCP and SAC algorithms. The legends of each sub figure are uniformly labeled in Figure(a)

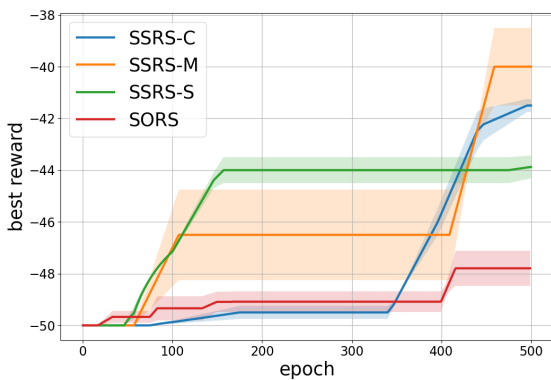


Figure 4: This figure shows the best score curve of SSRLS variants and aforementioned baseline over 500 epochs in the robotic manipulation environment FetchReach (mean \pm std over 3 seeds).

this deviates from the actual reward distribution of the environment, causing the reward estimator to degrade into a binary classifier. Experimental results also indicate a performance drop without the constraint. In contrast, SSRLS with a monotonicity constraint shapes a reward distribution that closely approximates the true reward distribution while also exhibiting the properties of a positively skewed normal distribution.

Feasibility of Semi-Supervised Learning

To further investigate why SSL method can infer rewards from trajectories more effectively than self-supervised methods—and why SSL techniques can be applied to reward shaping, we conduct the following experiment and analyses. We examine the trajectory distribution and obtain the consensus matrix \mathcal{C} in Figure 6. Each element $a_{ij} \in \mathcal{C}, 0 \leq a_{ij} \leq 1$, is frequency at which the two trajectories τ_i and τ_j are assigned to the same shaped reward value. Note that we use estimated reward values for labels.

Larger estimated reward values, i.e., rewards given for achieving long-term goals, exhibit clearer diagonal boundaries compared to smaller reward values. However, the decision boundaries inside high reward values are more am-

biguous, with only one clear diagonal block, aligning with the clustering assumption of SSL. SSL methods relies on the smoothness assumption and clustering assumption (Yang et al. 2023) on the augmented data, in this case, the trajectories. To be specific, for classification models, the smoothness assumption indicates if two points x_1, x_2 reside in a high-density region are close, then so should be their corresponding outputs y_1, y_2 . And clustering assumption indicates that samples from the same class are closer to each other, while there are significant boundaries between samples from different classes and the decision boundary of the model should be as far as possible from regions of high data density. Notably, this observed ambiguity in high reward values has minimal practical impact on SSRLS, as the reward estimator outputs these high rewards with negligible confidence probabilities.

Unlike conventional data augmentation techniques that may introduce excessive perturbations to non-image data—violating the smoothness and clustering assumptions—double entropy augmentation better preserves these assumptions in trajectory space. This is crucial to the step of calculating estimated reward, where the V network and Q network are not able to separate trajectories to learn a good representation of the space. From the perspective of the teacher-student model (Tarvainen and Valpola 2017), such a ‘muddled’ teacher would lead the student, *i.e.* policy module, to learn an unstable policy.

By also referring to Figure 5, it can be observed that the three ‘phases’ of significance in the consensus matrix plot correspond to the downward trend of the reward distribution probability. This can be understood from the perspective that as the estimated reward value increases, the randomness of the trajectory decreases, leading to greater clustering significance in the trajectory space, and *vice versa*.

Conclusion

In this paper, we propose a Semi-Supervised Reward Shaping (SSRLS) framework which utilizes zero reward trajectories by employing SSL technique. Additionally, we propose the double entropy data augmentation method for consistency regularization and a monotonicity constraint over modules of reward estimator. Our model outperforms previous supervised-based RCP and SORS methods in Atari environments, with a maximum of twice increase in reach-

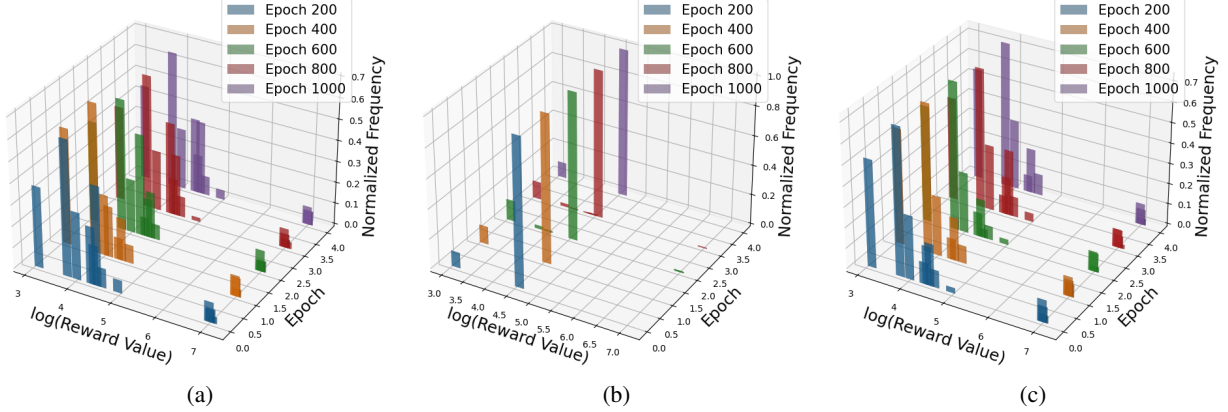


Figure 5: (a) represents SSRS with a monotonicity constraint, (b) represents SSRS without a monotonicity constraint, and (c) represents the baseline algorithm DQN. Shaped rewards from the buffer \mathcal{D} were sampled at epochs 200, 400, 600, 800, and 1000. Since the reward value distribution is sparse, the logarithm of the reward values is used as the x-axis, the y-axis represents values of epoch scale to 1/200, and the z-axis represents the normalized reward distribution probability.

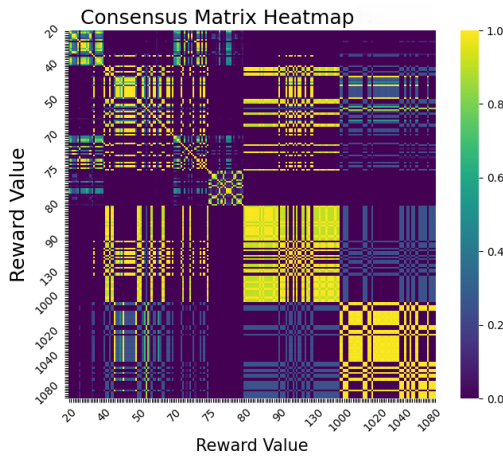


Figure 6: This figure shows the consensus matrix of reward distribution in Hero after 1000 episodes iterations, which indicates that the distribution of trajectories along the reward dimension in the trajectory space exhibits a certain clustering property. The cluster method used is Gaussian Mixture Models, and the number of iterations for consensus matrix is 100.

ing higher best scores. Moreover, the double entropy data augmentation enhances performance showcasing a 15.8% increase in best score compared to other augmentation methods. With SSL techniques, we can deploy agents on significantly sparser trajectory data. From a reverse perspective, it is possible to obtain learnable trajectories by artificially annotating rewards for a minimal number of transitions within a large set of trajectory data.

Moreover, it's worth noting that SSRS also introduces

several hyperparameters, such as the update probability of trajectories in the experience replay buffer p_u . Although the tuning of these hyperparameters has been studied in the literature of SSL, these hyperparameters can still provide valuable insights for the field of reinforcement learning. In this class of reward shaping algorithms, the tuning of p_u reflects the balance between exploration and exploitation in that, a higher p_u encourages the agent to exploit knowledge learned from the reward function, while a lower p_u prompts the agent to explore according to its original policy. Similar issues were also highlighted in Peng et al. (2019); Kumar, Peng, and Levine (2019), where the problem of controlling the reward shaping ratio arises. Like our paper, the balance shifts towards deciding whether the agent should exploit the reward from the estimator or prioritize exploration. We believe that a theoretical analysis of the dynamic relationship between the optimality of the estimator and the exploration-exploitation ratio would be a valuable direction for future work.

References

Andrychowicz, M.; Wolski, F.; Ray, A.; Schneider, J.; Fong, R.; Welinder, P.; McGrew, B.; Tobin, J.; Pieter Abbeel, O.; and Zaremba, W. 2017. Hindsight experience replay. *Advances in Neural Information Processing Systems*, 30.

Bachman, P.; Alsharif, O.; and Precup, D. 2014. Learning with pseudo-ensembles. In *Proceedings of the 28th International Conference on Neural Information Processing Systems - Volume 2*, NIPS'14, 3365–3373. Cambridge, MA, USA: MIT Press.

Bellemare, M. G.; Naddaf, Y.; Veness, J.; and Bowling, M. 2013. The Arcade Learning Environment: An Evaluation Platform for General Agents. *Journal of Artificial Intelligence Research*, 47: 253–279.

Bellemare, M. G.; Srinivasan, S.; Ostrovski, G.; Schaul, T.; Saxton, D.; and Munos, R. 2016. Unifying Count-Based

Exploration and Intrinsic Motivation. In *Neural Information Processing Systems*.

Berthelot, D.; Carlini, N.; Goodfellow, I.; Oliver, A.; Paper-
not, N.; and Raffel, C. 2019. *MixMatch: a holistic approach to semi-supervised learning*. Red Hook, NY, USA: Curran
Associates Inc.

Bricken, T. 2021. github/TrentBrick/RewardConditionedUDRL. Accessed: 2025-01-25.

Choi, J.; Guo, Y.; Moczulski, M.; Oh, J.; Wu, N.; Norouzi, M.; and Lee, H. 2019. Contingency-Aware Exploration in Reinforcement Learning. In *7th International Conference on Learning Representations, ICLR 2019, New Orleans, LA, USA, May 6-9, 2019*. OpenReview.net.

Gu, S.; Holly, E.; Lillicrap, T.; and Levine, S. 2017. Deep reinforcement learning for robotic manipulation with asynchronous off-policy updates. In *2017 IEEE international conference on robotics and automation (ICRA)*, 3389–3396. IEEE.

Haarnoja, T.; Zhou, A.; Hartikainen, K.; Tucker, G.; Ha, S.; Tan, J.; Kumar, V.; Zhu, H.; Gupta, A.; Abbeel, P.; and Levine, S. 2019. Soft Actor-Critic Algorithms and Applications. *arXiv:1812.05905*.

Hansen, N.; and Wang, X. 2020. Generalization in Reinforcement Learning by Soft Data Augmentation. *2021 IEEE International Conference on Robotics and Automation (ICRA)*, 13611–13617.

Hiwonjoon. 2021. [github/hiwonjoon/IROS2021_SORS](https://github.com/hiwonjoon/IROS2021_SORS). https://github.com/hiwonjoon/IROS2021_SORS. Accessed: 2025-01-25.

Kober, J.; Bagnell, J. A.; and Peters, J. 2013. Reinforcement learning in robotics: A survey. *The International Journal of Robotics Research*, 32: 1238 – 1274.

Kumar, A.; Peng, X. B.; and Levine, S. 2019. Reward-
Conditioned Policies. *ArXiv*, abs/1912.13465.

Lee, D.-H. 2013. Pseudo-Label : The Simple and Efficient Semi-Supervised Learning Method for Deep Neural Networks. *ICML 2013 Workshop : Challenges in Representation Learning (WREPL)*.

Lillicrap, T. P.; Hunt, J. J.; Pritzel, A.; Heess, N. M. O.; Erez, T.; Tassa, Y.; Silver, D.; and Wierstra, D. 2015. Continuous control with deep reinforcement learning. *CoRR*, abs/1509.02971.

Lin, Y.; Huang, J.; Zimmer, M.; Guan, Y.; Rojas, J.; and Weng, P. 2019. Invariant Transform Experience Replay: Data Augmentation for Deep Reinforcement Learning. *IEEE Robotics and Automation Letters*, 5: 6615–6622.

Memarian, F.; Goo, W.; Lioutikov, R.; Topcu, U.; and Niekum, S. 2021. Self-Supervised Online Reward Shaping in Sparse-Reward Environments. *2021 IEEE/RSJ International Conference on Intelligent Robots and Systems (IROS)*, 2369–2375.

Ng, A.; Harada, D.; and Russell, S. J. 1999. Policy Invariance Under Reward Transformations: Theory and Application to Reward Shaping. In *International Conference on Machine Learning*.

Ostrovski, G.; Bellemare, M. G.; van den Oord, A.; and Munos, R. 2017. Count-based exploration with neural density models. In *Proceedings of the 34th International Conference on Machine Learning - Volume 70*, ICML’17, 2721–2730. JMLR.org.

Pathak, D.; Agrawal, P.; Efros, A. A.; and Darrell, T. 2017. Curiosity-Driven Exploration by Self-Supervised Prediction. *2017 IEEE Conference on Computer Vision and Pattern Recognition Workshops (CVPRW)*, 488–489.

Peng, X. B.; Kumar, A.; Zhang, G.; and Levine, S. 2019. Advantage-Weighted Regression: Simple and Scalable Off-Policy Reinforcement Learning. *ArXiv*, abs/1910.00177.

Plappert, M.; Andrychowicz, M.; Ray, A.; McGrew, B.; Baker, B.; Powell, G.; Schneider, J.; Tobin, J.; Chociej, M.; Welinder, P.; Kumar, V.; and Zaremba, W. 2018. Multi-
Goal Reinforcement Learning: Challenging Robotics Environments and Request for Research. *ArXiv*, abs/1802.09464.

Riedmiller, M. A.; Hafner, R.; Lampe, T.; Neunert, M.; De-
grave, J.; de Wiele, T. V.; Mnih, V.; Heess, N. M. O.; and Springenberg, J. T. 2018. Learning by Playing - Solving Sparse Reward Tasks from Scratch. In *International Conference on Machine Learning*.

Sajjadi, M.; Javanmardi, M.; and Tasdizen, T. 2016. Regularization with stochastic transformations and perturbations for deep semi-supervised learning. In *Proceedings of the 30th International Conference on Neural Information Processing Systems*, NIPS’16, 1171–1179. Red Hook, NY, USA: Curran Associates Inc. ISBN 9781510838819.

Schaul, T.; Quan, J.; Antonoglou, I.; and Silver, D. 2015. Prioritized Experience Replay. *CoRR*, abs/1511.05952.

Shannon, C. E. 1948. A mathematical theory of communication. *Bell Syst. Tech. J.*, 27: 623–656.

Shorten, C.; and Khoshgoftaar, T. M. 2019. A survey on Image Data Augmentation for Deep Learning. *Journal of Big Data*, 6: 1–48.

Silver, D.; Huang, A.; Maddison, C. J.; Guez, A.; Sifre, L.; van den Driessche, G.; Schrittwieser, J.; Antonoglou, I.; Panneershelvam, V.; Lanctot, M.; Dieleman, S.; Grewe, D.; Nham, J.; Kalchbrenner, N.; Sutskever, I.; Lillicrap, T. P.; Leach, M.; Kavukcuoglu, K.; Graepel, T.; and Hassabis, D. 2016. Mastering the game of Go with deep neural networks and tree search. *Nature*, 529: 484–489.

Sohn, K.; Berthelot, D.; Li, C.-L.; Zhang, Z.; Carlini, N.; Cubuk, E. D.; Kurakin, A.; Zhang, H.; and Raffel, C. 2020. FixMatch: simplifying semi-supervised learning with consistency and confidence. In *Proceedings of the 34th International Conference on Neural Information Processing Systems*, NIPS’20. Red Hook, NY, USA: Curran Associates Inc. ISBN 9781713829546.

Tarvainen, A.; and Valpola, H. 2017. Mean teachers are better role models: Weight-averaged consistency targets improve semi-supervised deep learning results. In *Proceedings of the 31st International Conference on Neural Information Processing Systems*, NIPS’17, 1195–1204. Red Hook, NY, USA: Curran Associates Inc. ISBN 9781510860964.

Wang, C.; Wang, J.; Wang, J.; and Zhang, X. 2020. Deep-Reinforcement-Learning-Based Autonomous UAV Navigation With Sparse Rewards. *IEEE Internet of Things Journal*, 7: 6180–6190.

Weng, J.; Chen, H.; Yan, D.; You, K.; Duburcq, A.; Zhang, M.; Su, Y.; Su, H.; and Zhu, J. 2022. Tianshou: A Highly Modularized Deep Reinforcement Learning Library. *Journal of Machine Learning Research*, 23(267): 1–6.

Yang, X.; Song, Z.; King, I.; and Xu, Z. 2023. A Survey on Deep Semi-Supervised Learning. *IEEE Trans. on Knowl. and Data Eng.*, 35(9): 8934–8954.

Yarats, D.; Fergus, R.; Lazaric, A.; and Pinto, L. 2022. Mastering Visual Continuous Control: Improved Data-Augmented Reinforcement Learning. In *The Tenth International Conference on Learning Representations, ICLR 2022, Virtual Event, April 25-29, 2022*. OpenReview.net.

Yarats, D.; Kostrikov, I.; and Fergus, R. 2021. Image Augmentation Is All You Need: Regularizing Deep Reinforcement Learning from Pixels. In *9th International Conference on Learning Representations, ICLR 2021, Virtual Event, Austria, May 3-7, 2021*. OpenReview.net.

Double Entropy Data Augmentation

We introduce the proposed double entropy data augmentation here. *Shannon Entropy* (Shannon 1948) quantifies the amount of information required to describe or encode a random variable’s possible states. In RL tasks, observations and trajectories are matrices in practice, but can also be normalized and viewed as discrete random variable. Consider a $m \times n$ matrix A with each element $a_{ij} \geq 0$, $\forall i = 1, \dots, m$, $j = 1, \dots, n$, and the *Shannon Entropy* of matrix A is defined by

$$H(A) := - \sum_{k=1}^{mn} p_k \log(p_k), \quad (6)$$

where the probabilities are normalized by the matrix elements as $p_k = a_{ij} / \sum_i^m \sum_j^n a_{ij}$, such that $\sum_{k=1}^{mn} p_k = 1$.

Denote state space as $\mathcal{S} \in \mathbb{R}^{m_1}$ and action space as $\mathcal{A} \in \mathbb{R}^{m_2}$, with $m_1, m_2 \geq 1$. Consider a trajectory τ of length N as $\langle s_0, a_0, r_0, s_1, a_1, r_1, \dots, s_N \rangle$ with $a_t \in \mathcal{A}$, $s_t \in \mathcal{S}$, for all $t = 1, \dots, N$, and rewards are given following the environment’s original reward function $r_t = R(s_t, a_t, s'_t)$.

The set of all trajectories can be stacked into the matrix $\bar{\Gamma} = [S, A, R]$ with $S \in \mathbb{R}^{N \times m_1}$, $A \in \mathbb{R}^{N \times m_2}$ and $R \in \mathbb{R}^{N \times 1}$, and now we define the transform double entropy data augmentation σ over matrix $\bar{\Gamma}$ as:

$$\sigma(\bar{\Gamma}|n) := [[h^1 \cdot s^1, h^2 \cdot s^2, \dots, h^n \cdot s^n], A, R],$$

where $h^n \in \mathbb{R}$, equals to the entropy $H(s^n)$, matrix s^n is a submatrix of the stacked state S , obtained by equally dividing S into n parts along the state dimension. Here n is a hyperparameter.

Comparison of Data Augmentation Methods

Various types of data augmentation methods are used in the process of *consistency regularization*. Since the transformation double entropy data augmentation is thoroughly stated in previous section, we here list other transformation operations for data augmentation strategies involved in our experiment in Table 2 for completeness. Regarding to the heterogeneous SSRS variants which apply two weak and strong data augmentations in *consistency regularization*, the transformation details of the legends in Figures 3 in main text are listed below:

- **SSRS-S:** SSRS-S applies random Gaussian noise with standard deviation σ as the weak augmentation and double entropy data augmentation as strong augmentation.
- **SSRS-M:** SSRS-M applies σ random gaussian noise as the weak augmentation and smooth data augmentation as strong augmentation.
- **SSRS-C:** SSRS-C applies σ random gaussian noise as the weak augmentation and cutout data augmentation as strong augmentation.

The experiments in the paper are conducted on a Windows platform with an Intel i5-13400F and an Nvidia RTX 5060. The dependencies and libraries required for each task

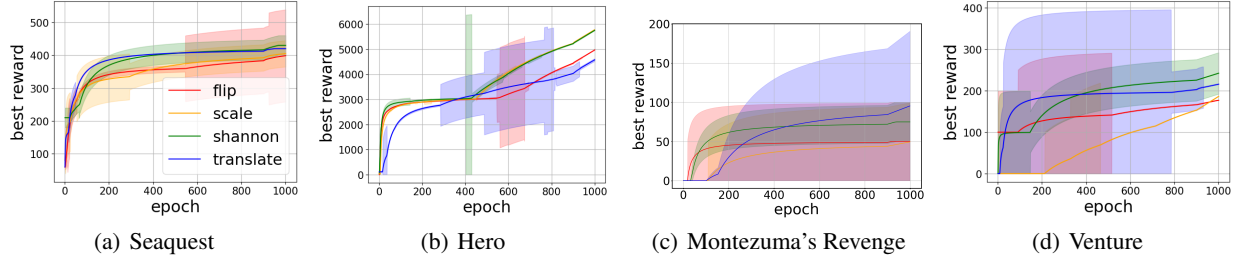


Figure 7: Figures (a–d) demonstrate the best score (mean \pm std over 3 seeds) in 1000 epochs of different data augmentation methods in 4 Atari environments. Note that Shannon refers to double entropy data augmentation. The legends of each sub figure are uniformly labeled in Figure(a)

Table 2: Data augmentation methods in the control group and SSRS variants. Weak augmentation is gaussian augmentation by default, and the rest augmentations are used as strong augmentations respectively.

TRANSFORMATION	DESCRIPTION	PARAMETER	RANGE
GAUSSIAN	ADD σ RANDOM GAUSSIAN NOISE TO THE OBSERVATION	σ	default = 0.1
CUTOUT	RANDOMLY ZERO OUT n COLUMNS OF OBSERVATION	n	default = 16
SMOOTH	SMOOTH n CONSECUTIVE OBSERVATIONS	n	default = 3
SCALE	SCALE THE OBSERVATION BY RANDOM SCALE FACTOR λ	λ	(0.8, 1.2)
TRANSLATION	HORIZONTALLY TRANSLATE THE OBSERVATION BY FACTOR λ	λ	(0, 0.1)
FLIP	HORIZONTALLY MIRROR FLIP THE OBSERVATION		

can be found in the code appendix. Here we give the supplementary material and analysis regarding to the experiment section. Figure 7 presents the performance of SSRS when employing different data augmentation methods as SSL perturbation, including our proposed double entropy data augmentation (labeled as "shannon" in the legend), along with conventional augmentation techniques such as flip, scale, and translate. In the first two games, Seaquest and Hero, double entropy data augmentation consistently maintains a leading position in terms of both convergence speed and final highest rewards, with the variance of the best reward remaining within a narrow range. In the more reward-sparse environment of MontezumaRevenge, although the final best reward achieved by the translate augmentation (blue curve) method is higher, it exhibits significantly larger variance. In contrast, double entropy data augmentation (green curve) demonstrates much smaller variance (Figure 7(c)), indicating a more stable policy and a faster update rate. In Venture, double entropy data augmentation maintains stable variance throughout (Figure 7(d)), whereas other data augmentation methods struggle to avoid larger variance in such a sparse environment, where disturbance to the data exceeded the decision-making boundaries of the trajectory space. Moreover, double entropy data augmentation achieves a best score that was 10 percentage points higher than the best result among tested image-based data augmentation methods in this environment.

Hyperparameters Settings

The hyperparameter setup of our experiments consists of the data augmentation parameters, the SSRS framework parameters and other general configurations. As for data augmen-

tation parameters, we adopt consistent settings throughout the experiments. Due to different environments, the shapes of states and observations are different, so the parameter n of double entropy data augmentation and cutout data augmentation, which is related to the state and observation dimension, are different in Atari and Robotic environments (see Table 3).

Table 3: The explicit value of n of aforementioned transformations in two environments. Note that Double-Ent refers to double entropy data augmentation.

VALUE OF n	DOUBLE-ENT	CUTOUT
ATARI	8	16
ROBOTIC	4	3

In Table 4, we present the settings of hyperparameters in SSRS framework, which are based on preliminary hyperparameter tuning results. Note that dynamic setting is applied to the consistency coefficient α and the threshold of confidence λ , *i.e.*, the value of these hyperparameters change during the training process, and the value shown in the Table 4 is the final value of the dynamic setting. In detail, the confidence threshold λ grows along with the training process. In a training process with T episodes in total, λ is as followed at the t episode:

$$\lambda = 0.6 + 0.3 \times \left(1 - e^{-\frac{t}{T}}\right)$$

Similarly, in a training process with T episodes in total, the

consistency coefficient α is as followed at the t episode:

$$\alpha = \begin{cases} 0.2 + (0.7 - 0.2) \times \left(\frac{t}{T \times 0.8}\right), & \text{if } t < 0.8 \cdot T \\ 0.7, & \text{otherwise} \end{cases}$$

The network architecture, training parameters, and other hyperparameters used in the experiments for the base SAC and DDPG algorithms follow the settings provided by the Tianshou RL Library (Weng et al. 2022) and paper Haarnoja et al. (2019); Lillicrap et al. (2015). Note the critic network shares the same hidden size with actor network and we only detail the actor network in Table 5. The hyperparameter settings of RCP refer to the settings in the code base (Bricken 2021) and paper (Kumar, Peng, and Levine 2019). The hyperparameter settings of SORS refer to the settings in the code base (Hiwonjoon 2021) and paper (Memarian et al. 2021). Additionally, the network architecture of the reward estimator is also presented in Table 5.

The Gradients of Loss Functions

The Gradient of L_{QV}

The L_{QV} has the following explicit form:

$$L_{QV} = \begin{cases} 0, & \delta_t(\theta) < 0, \\ \frac{1}{\mu B} \sum_{t=1}^{\mu B} (\delta_t(\theta))^2, & \text{else.} \end{cases} \quad (7)$$

Denote $\delta_t(\theta) = Q(s_t, a_t, \theta_1) - V(s_t, \theta_2)$, where θ is the combination of θ_1 and θ_2 . Consider a batch of size B , within which a proportion $\mu_l \geq 0$ of the samples satisfy $\delta_t(\theta) < 0$. The remaining proportion $(1 - \mu_l)$ contributes to the gradient with respect to the parameter $\theta = (\theta_1, \theta_2)$ is given by:

$$\begin{aligned} \frac{\partial L_{QV}}{\partial \theta} = \frac{2}{(1 - \mu_l)B} \sum_{t \in \mathcal{I}_+} & \left(Q(s_t, a_t, \theta_1) - V(s_t, \theta_2) \right) \\ & \cdot \begin{bmatrix} \nabla_{\theta_1} Q(s_t, a_t, \theta_1) \\ -\nabla_{\theta_2} V(s_t, \theta_2) \end{bmatrix}. \end{aligned}$$

Here, \mathcal{I}_+ denotes the set of indices for which $Q(s_t, a_t, \theta_1) - V(s_t, \theta_2) \geq 0$.

The Gradient of L_r

Consider loss function L_r in Eq.(3) as follow:

$$L_r = \frac{1}{\mu B} \sum_{t=1}^{\mu B} \mathbb{1}(\max(\mathbf{q}_t) \geq \lambda) (r_t - \alpha(\mathbf{q}_t, \lambda))^2,$$

where confidence score $\mathbf{q}_t = \beta Q(s_t, a_t, \theta_1) + (1 - \beta)V(s_{t+1}, \theta_2)$. Note that the indicator function $\mathbb{1}(\max(\mathbf{q}_t) \geq \lambda)$ is not differentiable due to its discontinuity at the boundary of $\max(\mathbf{q}_t) \geq \lambda$. The derivative of the indicator function only has non-zero contribution at the boundary, i.e. $\max(\mathbf{q}_t) = \lambda$. In order to derive the gradient of L_r , we approximate the indicator function $\mathbb{1}(\max(\mathbf{q}_t) \geq \lambda)$ using differentiable function, for simplicity, the sigmoid function, achieving the effect of approximate binary selection:

$$\mathbb{1}(\max(\mathbf{q}_t) \geq \lambda) \approx \sigma(\max(\mathbf{q}_t) - \lambda),$$

where the sigmoid function $\sigma(x)$ is defined as:

$$\sigma(x) = \frac{1}{1 + \exp(-x)}. \quad (8)$$

Thus, the loss function becomes:

$$L_r = \frac{1}{\mu B} \sum_{t=1}^{\mu B} \sigma(\max(\mathbf{q}_t) - \lambda) (r_t - \alpha(\mathbf{q}_t, \lambda))^2.$$

We want to compute the gradient of L_r with respect to $\theta = (\theta_1, \theta_2)$. The loss function has two parts that depend on θ_1 and θ_2 : one is \mathbf{q}_t , and the other is $\alpha(\mathbf{q}_t, \lambda)$. The gradients of the former are:

$$\frac{\partial \mathbf{q}_t}{\partial \theta_1} = \beta \frac{\partial Q(s_t, a_t, \theta_1)}{\partial \theta_1}, \quad (9)$$

$$\frac{\partial \mathbf{q}_t}{\partial \theta_2} = (1 - \beta) \frac{\partial V(s_{t+1}, \theta_2)}{\partial \theta_2},$$

Thus, the loss function L_r can be rewritten as:

$$L_r = \frac{1}{\mu B} \sum_{t=1}^{\mu B} f_r e_t^2,$$

where f_r is the sigmoid function $\sigma(\max(\mathbf{q}_t) - \lambda)$ defined in Eq.(8) and $e_t = r_t - \alpha(\mathbf{q}_t, \lambda)$. The derivative of f_r with respect to θ_1 is:

$$\frac{\partial f_r}{\partial \theta_1} = \frac{\partial \sigma(\max(\mathbf{q}_t) - \lambda)}{\partial \max(\mathbf{q}_t)} \cdot \frac{\partial \max(\mathbf{q}_t)}{\partial \mathbf{q}_t} \cdot \frac{\partial \mathbf{q}_t}{\partial \theta_1} \quad (10)$$

Since $\frac{\partial \sigma(x)}{\partial x} = \sigma(x)(1 - \sigma(x))$, plugging it in Eq.(9), we get:

$$\begin{aligned} \frac{\partial f_r}{\partial \theta_1} = & \sigma(\max(\mathbf{q}_t) - \lambda)(1 - \sigma(\max(\mathbf{q}_t) - \lambda)) \\ & \cdot \frac{\partial \max(\mathbf{q}_t)}{\partial \mathbf{q}_t} \cdot \beta \frac{\partial Q(s_t, a_t, \theta_1)}{\partial \theta_1}. \end{aligned}$$

Similarly, we can also derive $\frac{\partial f_r}{\partial \theta_2}$. Now, the gradient of L_r with respect to θ_1 and θ_2 can be computed using the chain rule. The gradient with respect to θ_1 is:

$$\frac{\partial L_r}{\partial \theta_1} = \frac{1}{\mu B} \sum_{t=1}^{\mu B} \left[\frac{\partial f_r}{\partial \theta_1} e_t^2 + f_r \cdot 2e_t \cdot \frac{\partial \alpha(\mathbf{q}_t, \lambda)}{\partial \theta_1} \right].$$

Similarly, for θ_2 , the gradient is:

$$\frac{\partial L_r}{\partial \theta_2} = \frac{1}{\mu B} \sum_{t=1}^{\mu B} \left[\frac{\partial f_r}{\partial \theta_2} e_t^2 + f_r \cdot 2e_t \cdot \frac{\partial \alpha(\mathbf{q}_t, \lambda)}{\partial \theta_2} \right].$$

Thus, we have derived the gradient of the loss function L_r with respect to θ_1 and θ_2 , taking into account the sigmoid approximation of the indicator function.

Table 4: The setting of hyperparameters in SSRS framework.

HYPERPARAMETER	DESCRIPTION	VALUE
β	THE QV CONFIDENCE COEFFICIENT	0.5
λ	THE THRESHOLD OF CONFIDENCE	0.9
α	THE CONSISTENCY COEFFICIENT	0.7
p_u	THE UPDATE PROBABILITY	0.01
N_z	THE SIZE OF THE FIXED REWARD SET Z	12
n	PARTITION NUMBER OF DOUBLE ENTROPY AUGMENTATION	8

The Gradient of L_s

The loss function L_s is:

$$L_s = \frac{1}{(1-\mu)B} \sum_{t=1}^{(1-\mu)B} [\mathbb{1}(\max(\mathbf{q}_t^s) \geq \lambda, \max(\mathbf{q}_t^w) \geq \lambda) \times \mathcal{H}(\mathbf{q}_t^{w,'}, \mathbf{q}_t^{s,'})].$$

To compute $\partial L_s / \partial \theta_1$, we will apply the chain rule. The loss L_s involves a sum of products, and we need to consider the parts that depend on θ_1 . We adopt the same approach, using sigmoid function (see Eq.(8)) approximation for the indicator function. Therefore, the overall approximation of the indicator function is:

$$\begin{aligned} & \mathbb{1}(\max(\mathbf{q}_t^s) \geq \lambda, \max(\mathbf{q}_t^w) \geq \lambda) \\ & \approx \sigma(\max(\mathbf{q}_t^s) - \lambda) \cdot \sigma(\max(\mathbf{q}_t^w) - \lambda). \end{aligned} \quad (11)$$

The approximate derivative of the indicator function $\mathbb{1}(\max(\mathbf{q}_t^s) \geq \lambda, \max(\mathbf{q}_t^w) \geq \lambda)$ (denoted as f_s) with respect to θ_1 is computed based on Eq.(10) and Eq.(11):

$$\begin{aligned} \frac{\partial f_s}{\partial \theta_1} &= \sigma(\max(\mathbf{q}_t^s) - \lambda)(1 - \sigma(\max(\mathbf{q}_t^s) - \lambda)) \\ &\quad \cdot \sigma(\max(\mathbf{q}_t^w) - \lambda) \cdot \frac{\partial \max(\mathbf{q}_t^s)}{\partial \theta_1} \\ &\quad + \sigma(\max(\mathbf{q}_t^s) - \lambda) \cdot \sigma(\max(\mathbf{q}_t^w) - \lambda) \\ &\quad \cdot (1 - \sigma(\max(\mathbf{q}_t^w) - \lambda)) \cdot \frac{\partial \max(\mathbf{q}_t^w)}{\partial \theta_1}. \end{aligned} \quad (12)$$

Then, compute the derivative of the cross-entropy with respect to θ_1 . The cross-entropy between two distributions p and q is given by:

$$\mathcal{H}(p, q) = - \sum_i p_i \log(q_i)$$

where p_i are the true probabilities and q_i are the predicted probabilities. Since $\mathbf{q}_t^{w,'}$ is a one-hot encoded vector, where only one position is 1 and others are 0, the cross-entropy in Eq.(5) is simplified to:

$$\mathcal{H}(p, q) = - \log(q_{i^*})$$

where i^* is the index where $q_1^{w,'} = 1$. Therefore, by chain rule the derivative of the cross-entropy with respect to θ_1 is:

$$\begin{aligned} \frac{\partial \mathcal{H}(p, q)}{\partial \theta_1} &= \frac{\partial \mathcal{H}(p, q)}{\partial q_{i^*}} \cdot \frac{\partial q_{i^*}}{\partial \theta_1} \\ &= -\frac{1}{q_{i^*}} \cdot \frac{\partial q_{i^*}}{\partial \theta_1} \end{aligned} \quad (13)$$

The loss L_s involves a sum of products, and now that we have derived the parts that depend on θ_1 in Eq.(12) and Eq.(13), the gradient of the loss function with respect to θ_1 is:

$$\begin{aligned} \frac{\partial L_s}{\partial \theta_1} &= \frac{1}{(1-\mu)B} \sum_{t=1}^{(1-\mu)B} \left[\frac{\partial f_s}{\partial \theta_1} \cdot \mathcal{H}(\mathbf{q}_t^{w,'}, \mathbf{q}_t^{s,'}) \right. \\ &\quad \left. - f_s \cdot \frac{1}{q_{i^*}} \cdot \frac{\partial q_{i^*}}{\partial \theta_1} \right]. \end{aligned}$$

where $\frac{\partial f_s}{\partial \theta_1}$ refers to Eq.(12).

Similarly, we can derive the gradient of L_s with respect to θ_2 .

Table 5: Network architecture and hyperparameters

ARCHITECTURE AND HYPERPARAMETERS		VALUE
ACTOR NETWORK	- CONV(32-8x8-4) / RELU	
	- CONV(64-4x4-2) / RELU	
	- CONV(64-3x3-1) / RELU	
	- FLATTEN	
	- FC(512) / RELU	
	- FC(—A—)	
	- FC(128) / RELU	
	- DROPOUT(P=0.2)	
	- FC(64) / RELU	
	- DROPOUT(P=0.2)	
REWARD NETWORK	- FC(32) / RELU	
	- DROPOUT(P=0.2)	
	- FC(N_z) / RELU	
	- SOFTMAX(DIM=-1)	
	DISCOUNT FACTOR γ	0.99
	ACTOR LEARNING RATE	0.001
	CRITIC LEARNING RATE	0.001
DDPG	BATCH SIZE	256
	NUMBER OF PARALLEL ENVIRONMENTS	8
	UPDATE PER STEP	1
	SOFT UPDATE τ	0.005
	EXPLORATION NOISE	0.1
SAC	ENTROPY COEFFICIENT α	0.05
	AUTO-ALPHA	TRUE
	ALPHA LEARNING RATE	0.0003
RCP	β REWARD WEIGHTING	1
	MAX LOSS WEIGHTING	20
	TD λ	0.95
SORS	REWARD UPDATE PERIOD	1000
	REWARD UPDATE NUM	100
	REWARD BATCH SIZE	10